

Green Chemistry

Cutting-edge research for a greener sustainable future

Accepted Manuscript

View Article Online
View Journal

This article can be cited before page numbers have been issued, to do this please use: C. Cova, A. Zuliani, R. Manno, V. Sebastian and R. Luque, *Green Chem.*, 2020, DOI: 10.1039/C9GC04091A.



This is an Accepted Manuscript, which has been through the Royal Society of Chemistry peer review process and has been accepted for publication.

Accepted Manuscripts are published online shortly after acceptance, before technical editing, formatting and proof reading. Using this free service, authors can make their results available to the community, in citable form, before we publish the edited article. We will replace this Accepted Manuscript with the edited and formatted Advance Article as soon as it is available.

You can find more information about Accepted Manuscripts in the [Information for Authors](#).

Please note that technical editing may introduce minor changes to the text and/or graphics, which may alter content. The journal's standard [Terms & Conditions](#) and the [Ethical guidelines](#) still apply. In no event shall the Royal Society of Chemistry be held responsible for any errors or omissions in this Accepted Manuscript or any consequences arising from the use of any information it contains.

ARTICLE

Scrap waste automotive converters as efficient catalysts for the continuous-flow hydrogenations of biomass derived chemicals

Camilla Maria Cova,^a Alessio Zuliani,^a Roberta Manno,^b Victor Sebastian^{b,c,d} and Rafael Luque^{*a,e}Received 00th January 20xx,
Accepted 00th January 20xx

DOI: 10.1039/x0xx00000x

The catalytic activity of the scrap ceramic-core of automotive catalytic converters (SCATs) was investigated in the continuous-flow hydrogenation of different biomass-derived chemicals. The waste SCATs powders were deeply characterized by ICP-MS, TGA, MP-AES, XRD, N₂ physisorption, TPR, HRTEM and EDS before and after the utilization as catalyst. The hydrogenation reactions of isopulegol to menthol; cinnamyl alcohol to hydrocinnamyl alcohol; isoeugenol to dihydroeugenol; vanillin to vanillyl alcohol and benzaldehyde to benzyl alcohol were performed studying the influence on of various reaction parameters (temperature, pressure, flow rate and concentration of the starting material) on the final yields. The outstanding performance and stability obtained for the low metal content of waste-derived catalysts can be attributed to the co-presence of different noble metals as well as to the composite structure itself.

1. Introduction

The design of inexpensive, selective and efficient catalytic materials with low-environmental impact is of primary importance for the development of sustainable industrial processes.^{1, 2} As a result, research has recently focused on the synthesis of alternative environmentally friendly catalysts having catalytic activity comparable to that of commercially available systems. For example, Fe-Ni supported on a natural zeolite has been proposed as alternative to noble metals for the cyclization of levulinic acid to γ -valerolactone.³ Also, Sun *et al.* designed a material based on CuNi nanoparticles assembled on graphene, as valid catalyst for the hydrogenation of nitro/nitrile compounds.⁴ More recently, Ni/ZrO₂ has shown good performances as catalyst for the selective hydrogenation of fatty acids to alkanes and alcohols.⁵

However, despite these promising results, the preparation of sustainable catalysts frequently has certain limitations including long preparation procedures or high production costs as well as the side production of high amount of waste (high E-Factor). Due to the content of noble metals and the presence of different inorganic composites, the peculiar structure of

ceramic-cores of catalytic converters (CATs) derived from end-of-life (ELV) vehicles offers a promising potential to be employed as catalyst. More in detail, the direct utilization of scrap ceramic-cores of CATs (denoted SCATs) as catalysts avoids the production of additional waste or the requirement of time-consuming processes. Furthermore, SCATs are largely available and cheap, making them potentially commercially competitive with traditional catalysts. In fact, every year, end-of-life vehicles (ELVs) generate *ca.* 8-9 million tons of valuable wastes in the European Union alone. The Directive 2000/53/EC, otherwise referred to as "ELV Directive", seeks to dismantle and recycle end-of-life vehicles through more sustainable and environmentally friendly procedures.⁶⁻⁷ The directive fixes specific targets for recovery, recycling and reuse of ELVs and their components. Between all ELVs valuable waste, around 6 thousand tons of ceramic cores of scrap automotive catalytic converters (SCATs) are yearly produced.

The catalytic activity of SCATs rises from the strong stability of the noble metals supported on the inorganic support. The honeycomb structure of SCATs is composed of four principal coats: the catalyst substrate, made of cordierite (2MgO·2Al₂O₃·5SiO₂), the wash coat (Al₂O₃, TiO₂, SiO₂ or SiO₂-Al₂O₃ mixture), functioning as a carrier for the catalytic material, a coat made of CeO₂ or CeO₂/ZrO₂ and a coat covered with noble metals in low loadings including platinum and palladium, and other metals, such as Fe, Mn, Ni and Ce.⁸⁻¹⁰

Currently, SCATs are normally processed in order to extract and recover the noble metals (Platinum group metals - PGMs). However, these methodologies require the use of large amounts of highly toxic chemicals (*i.e.* inorganic acids) and long treatment times.¹¹⁻¹⁵ Moreover, since only the noble metals are recovered, these processes generate extensive volumes of waste, as the SCATs matrix is not recycled. According to literature, R&D is nowadays generally limited on diminishing the utilization of inorganic acids or on enhancing the efficiency of

^a Departamento de Química Orgánica, Universidad de Córdoba, Edificio Marie-Curie (C-3), Ctra Nnal IV-A, Km 396, Córdoba, Spain. E-mail: rafael.luque@uco.es

^b Nanoscience Institute of Aragon and Chemical and Environmental Engineering Department, University of Zaragoza, 50018 Zaragoza, Spain

^c Networking Research Center CIBER-BBN, 28029 Madrid, Spain

^d Aragón Materials Science Institute, ICMA, CSIC – University of Zaragoza, Pedro Cerbuna 12, 50009 Zaragoza, Spain

^e Peoples Friendship University of Russia (RUDN University), 6 Miklukho Maklaya str., 117198, Moscow, Russia

[†]Electronic Supplementary Information (ESI) available: GC chromatogram graph of fluxed toluene in freshly made SCATs cartridge, TPR analysis of SCATs, ICP-MS analysis, BET isotherm and XRD patterns of SCATs, photos of the heating units of the H-Cube® and X-Cube™, GC-MS chromatogram graph of fluxed toluene in SCATs cartridge after stability test.

the extraction processes adding for example peroxides or using chelating agents.¹⁶⁻¹⁹ Only a few studies described SCATs as catalysts (*e.g.*, for the reduction of nitroarenes with NaBH_4) but the reactions to date have been strictly limited to batch conditions.²⁰⁻²²

In the present work, SCATs were exploited as cheap, efficient and environmentally friendly catalyst in a continuous flow hydrogenation system. To the best of our knowledge, no similar work has been previously described. In order to make SCATs suitable for continuous flow equipment, a first cleaning approach was necessary. Prior to the utilization, SCATs were in fact washed under ultrasonication and subjected to a thermal treatment in order to remove all surface residuals (gasoline, oils, *etc.*) and clean. Remarkably, the direct reutilization of SCATs as catalysts doesn't generate substantial additional waste (apart from the small amount of solvents used for the washing procedures), in significant contrast with metal extraction processes or costly metal/metal oxide catalyst preparations.

The continuous flow system was selected to explore the activity and particularly stability of SCATs in sustainable and cost-effective chemical synthesis. Indeed, flow-chemistry is one of the tools to achieve the United Nations Sustainable Development Goals (SDGs), whose target is reaching a greener and better future by 2030.²³ Also, the IUPAC has recently included flow chemistry between the top ten chemical innovations that will change our world in the future, with the potential to make our planet sustainable. Finally, continuous-flow reactors offer numerous advantages counting the reduction of consumption by using small volumes of solvents, the reduction of the risk of handling dangerous chemicals and the increased reaction selectivity and yields altogether with easy scaling-up, responding to some of the key principles of Green Chemistry (prevention of waste formation, less hazardous reactions, safer chemicals, *etc.*).²⁴⁻²⁹

In order to prove the practical utilization of SCATs as catalysts, different hydrogenations of biomass derived chemicals were performed.

In particular, the hydrogenation of (–)-isopulegol to (–)-menthol, widely used industrial synthesis, was chosen as the initial test reaction.³⁰⁻³¹ (–)-menthol (cooling minty flavor) is in fact one of the most important chemicals, with a large range of uses in pharmaceuticals, flavorings, cosmetics, agrochemicals and personal-care applications.³²⁻³⁷ Nowadays, (–)-menthol is principally synthesized through the myrcene process (Takasago process), which last two steps include the cyclization of citronellal and hydrogenation of isopulegol.³⁸⁻⁴⁰

Sequentially, the selective hydrogenations of other important biomass-derived chemical for the food and fragrances industries were performed, highlighting the operative conditions in order to maximise the final yields. More in details, the hydrogenation of cinnamyl alcohol to hydrocinnamyl alcohol (sweet, balsamic and spicy flavour); isoeugenol to dihydroeugenol (clove, spicy and peppery flavour); vanillin to vanillyl alcohol (sweet, vanilla and caramelly flavour) and benzaldehyde to benzyl alcohol (sweet, floral and fruity flavour) were explored.

2. Experimental Sections

View Article Online
DOI: 10.1039/C9GC04091A

Ethanol ($\geq 99.8\%$), acetone ($\geq 99.5\%$), (–)-isopulegol ($\geq 99\%$, enantiomeric ratio: $\geq 99.5:0.5$), (–)-menthol ($\geq 99\%$, enantiomeric ratio: $\geq 99.5:0.5$), cinnamyl alcohol (98%), hydrocinnamyl alcohol ($\geq 98\%$), isoeugenol (98%), dihydroeugenol ($\geq 99\%$), vanillin (99%), vanillyl alcohol ($\geq 98\%$), benzaldehyde ($\geq 99\%$), benzyl alcohol (99.8%) were purchased from Sigma-Aldrich Inc., St. Louis, MO, USA. All reagents were used without any further purification. Scrap ceramic-cores of automotive catalytic converters (SCATs) were collected from Provaluta España Reciclaje de Metales, S.L., Córdoba (ES). SCATs were previously smashed in Provaluta S.L. *via* a grinding process and provided in the form of powders.

2.1 SCATs preparation

Prior to the utilization as catalysts, the powders of scrap ceramic-cores of automotive catalytic converters (SCATs), kindly donated by the company PROVALUTA S.L., were washed and dried. Firstly, the powders were subjected to a sequence of washing cycles using hot water, ethanol, and acetone for 60' in a US bath. The washed powders were filtrated, dried and weighted after each cycle. When no loss of weight was observed, the washing cycles were stopped (5 cycles). A thermal treatment was sequentially performed in order to clean the surface of the metals and remove residuals.⁴¹ More in details, the powders were heated for 1 h under N_2 flux and for 3 h under 10%vol H_2 flux at 500 °C in a tubular furnace. Finally, the powders were cooled down to room temperature under N_2 stream.

2.2 SCATs characterization

The thermogravimetric analyses (TGA) were carried out with a Mettler Toledo TGA/SDTA 851 analyzer. The catalysts were heated from 25 °C up to 900 °C at 5 °C min^{-1} in nitrogen atmosphere (50 mL min^{-1}).

TPR (Temperature programmed reduction) analysis was performed with a ChemBET Pulsar TPR/TPD_Automated Chemisorption Analyzer (Quantachrome Instruments). The mesurment was performed operating under a 10% H_2 flux (in N_2) of 20 mL min^{-1} , heating the sample at 10 °C min^{-1} up to 900 °C.

Powder X-ray diffraction (XRD) pattern was recorded with a Bruker D8 DISCOVER A25 diffractometer (PanAnalytic/Philips, Lelyweg, Almelo, The Netherlands) using $\text{CuK}\alpha$ ($\lambda = 1.5418\text{\AA}$) radiation. Wide angle scanning patterns were collected over a 2θ range from 10° to 80° with a step size of 0.018° and counting time of 5 s per step.

Textural properties of the sample were determined by N_2 physisorption using a Micromeritics ASAP 2020 automated system (Micromeritics Instrument Corporation, Norcross, GA, USA) using the Brunauer-Emmet-Teller (BET) and the Barret-Joyner-Halenda (BJH) methods. The sample was outgassed for 24 h at 100 °C under vacuum ($P_0 = 10^{-2}$ Pa) and subsequently analysed.

The metallic composition of the catalysts adopted was determined by Microwave Plasma Atomic Emission Spectroscopy (MP-AES) (Agilent 4100 MP-AES). A representative analysis was carried out by digesting 20 mg of the catalyst with the addition of 5 mL of nitric acid (HNO₃) and hydrochloric acid (HCl) in a volume ratio of 1:3, the mixture was heated at 200 °C for 20 minutes in a microwave oven (Milestone Ethos Plus). The digested sample was diluted with Milli-Q water to obtain a final volume of 30 mL, after filtration by hydrophilic syringe filters of 0.2 µm to discard any fragmented particles. Aberration corrected scanning transmission electron microscopy (Cs-corrected STEM) images were acquired in a FEI XFEI TITAN electron microscope operated at 300 kV equipped with a CETCOR Cs-probe corrector from CEOS Company allowing formation of an electron probe of 0.08 nm. A 10 µL suspension of the sample was pipetted onto a TEM copper grid having a continuous carbon film. After complete evaporation, the sample was analyzed by High-angle annular dark-field scanning transmission electron microscopy (STEM-HAADF). Elemental analysis was carried out with an EDS (EDAX) detector which allows performing EDS experiments in the scanning mode. This analysis was conducted at the Laboratory of Advanced Microscopies, LMA-INA-University of Zaragoza.

2.3 Preparation of the cartridges

In order to perform the continuous flow tests, washed and thermally-treated SCATs were charged in 30 mm-long ThalesNano CatCarts® or in 70 mm-long ThalesNano CatCarts® sealed on both sides with sealings systems, made of graphite filled PTFE sealing rings, stainless steel filters and PTFE membranes (CatCarts® Thalesnano Inc.). The cartridges were filled with 200 mg of SCATs (in 30 mm-long ThalesNano CatCarts®) or 450 mg of SCATs (in 70 mm-long ThalesNano CatCarts®). The cartridges were sequentially charge in the hydrogenation systems and subjected to washing cycles with toluene. After the washing cycles, fresh fluxed toluene was analysed by GC (please see Fig. S1 in the ESI for a GC chromatogram graph) and ICP-MS analysis in order to confirm the cleanliness of the system and that no leaching of the catalysts occurred.

2.4 Catalytic experiments

Catalytic performances of the catalyst were evaluated under liquid phase continuous-flow conditions in an H-Cube® Mini Plus flow hydrogenation reactor. The material was packed (200 mg of SCATs per cartridge) in 30 mm-long ThalesNano CatCarts® or (450 mg of SCATs per cartridge) in 70 mm-long ThalesNano CatCarts®. The reaction solution in toluene was pumped through and the reaction conditions were setted. The required hydrogen was generated *in situ* during the reaction by water electrolysis in the H-Cube equipment. The reactions were performed for 120', collecting samples every 15' for further analysis.

Further hydrogenation trials were performed in a combined apparatus set up by linking an H-Cube® Mini Plus (Thalesnano Inc.) to an X-Cube™ (Thalesnano Inc.). More in details, the heating unit and the Cartridge holder of the instrument X-Cube™ were used, while the hydrogen was generated in the H-Cube® equipment. This set up allows to set and control the temperature by the X-Cube™ and the H₂ pressure and flow rate by the H-Cube®.

The conversion and selectivity were analyzed by gas chromatography (GC) in an Agilent 6890N gas chromatograph (60 mL min⁻¹ N₂ carrier flow, 20 psi column top head pressure) using a flame ionization detector (FID). A capillary column Agilent Technologies Inc. HP-5 (30 m × 0.32 mm × 0.25 µm) was employed. In the case of the hydrogenation of (–)-isopulegol, the formation of (–) menthol a capillary column Restek Rt®-yDEXsa (30 m × 0.25 mm × 0.25 µm) was employed. The retention times were confirmed using standards of the desired products. Calibration curve was obtained with an internal standard method using octane as standard. Standard solutions of (–)-isopulegol / cinnamyl alcohol / isoeugenol / vanillin / benzaldehyde (from 0.005 to 2 M) and octane in toluene were analyzed by GC to give linear regressions with R² > 0.999. In addition, the collected liquid fractions were analyzed by GC-MS—using the Agilent 7820A GC/5977B High Efficiency Source (HES) MSD—in order to identify and confirm the obtained products.

3. Results and discussion

3.1 Characterization of the catalysts

In order to evaluate the washing/thermal cleaning procedure and prove that no thermal leaching could occur during the hydrogenation reactions, thermal gravimetric analysis were performed on both the starting scrap core catalytic converter powder (SCATs) and on the washed and thermally treated SCAT, before and after utilization in the hydrogenation reactions. As shown in Fig. 1, the loss in weight of the starting SCATs heated up to 900 °C could be approximated to ~20%.

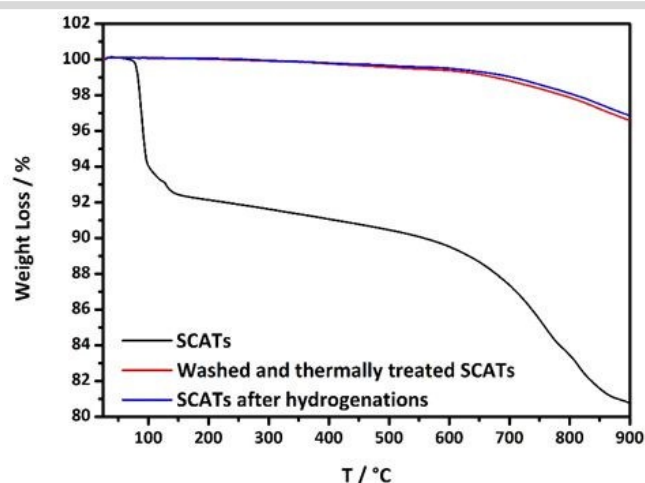


Fig. 1 TGA of starting SCATs, washed and thermally treated SCATs and washed and thermally treated SCATs after hydrogenation reactions.

On the other hand, after the washing and thermal cleaning procedure, the SCATs didn't show any relevant loss of weight (<4% of weight loss above 600 °C, not relevant for the operative hydrogenation conditions). Furthermore, the used SCATs had the same TGA profile of the freshly washed-thermal treated SCATs, proving that no relevant changes in the structure of the SCATs occurred.

Additional TPR analysis of both washed and thermally treated SCAT evidenced that the activation of the supported metals can be centered at ca. 500 °C (please see ESI Fig. S2 for details). Remarkably, this result demonstrated that is not possible to achieve an *in-situ* reduction of the metals under the operative flow reaction conditions.

The metallic composition of SCATs was determined by Inductively coupled plasma mass spectrometry (ICP-MS) and Microwave Plasma Atomic Emission Spectroscopy (MP-AES). Qualitative analysis of SCATs by ICP-MS revealed Al, Si and Mg as main components while also minor components such as Ce and Fe and traces of Pt (0.1-0.2 wt.%) were detected (for a complete qualitative analysis, please see ESI Table S1). A quantitative analysis by MP-AES allowed to specifically identify 0.68 wt.% of Fe, 3.01 wt.% of Ce and 0.10 wt.% of Pt in the freshly ground SCATs. Additionally, SCATs were also analysed after the catalytic tests. Considering the heterogeneity of the substrate, no relevant metallic leaching was observed.

Due to the low concentration, no specific peaks of the metals were detectable in XRD analysis, while most intense peaks were associated to SiO₂. No difference between XRD patterns before and after utilization were noticed (please see ESI Fig. S3 for XRD patterns).

Fig. 2 shows STEM-HAADF images and EDS analysis of SCATs before utilization.

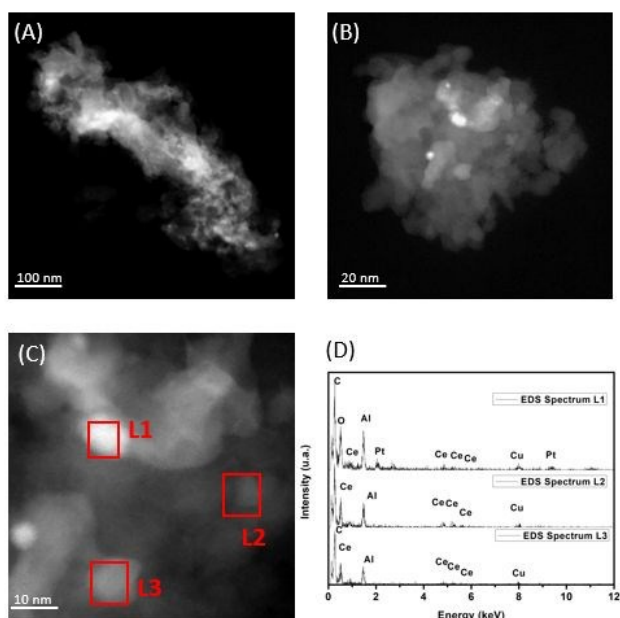


Fig. 2 (A), (B) and (C) STEM-HAADF images of SCATs. (D) EDS analysis of selected locations (L1-L3).

In the images reported in Fig. 2A, 2B and 2C, it is possible to observe the smashed laminar structures of SiO₂ and Al₂O₃ derived from the honeycomb structure of the catalytic converters. Bright contrast is observed for those atoms with high atomic number (Z contrast). Energy-dispersive X-ray spectroscopy analysis of selected surface areas, L1, L2 and L3 in Fig. 2C, can be associated with the presence of cerium oxide and Pt nanoparticles, as illustrated in Fig. 2D.

3.2 Hydrogenation tests

Preliminary studies: hydrogenation of (–)-isopulegol. The catalytic activity of SCATs was initially evaluated in an H-Cube® Mini Plus flow hydrogenation reactor. Washed and thermally treated SCATs were firstly packed (200 mg of powder per cartridge) in 30 mm-long cartridge ThalesNano CatCarts®. The hydrogenation of (–)-isopulegol to (–)-menthol was carried out using a solution 20 mM of (–)-isopulegol in toluene. The upper value of 100 °C was forced due to operative limitations of the equipment.

Firstly, a set of trials was performed fixing the reaction temperature at 100 °C and varying the H₂ pressure (from 10 to 40 bar). A higher pressure delivered a higher yield. As the yield obtained (Table 1, entry 5) at 40 bar of H₂ pressure was almost the same obtained at 30 bar (~91% of yield), as showed in Table 1, entry 4, this last value was chosen as reaction pressure, lowering the energy consumption.

Sequentially, a range of experiments were conducted operating at 30 bar H₂ pressure at different reaction temperature (75, 90 and 100 °C). Higher temperature provided higher yields, showing a linear trend. Indeed, at stationary state, (–)-menthol yields were 55.5%, 73.1% and 91.3% operating at 75, 90 and 100 °C, respectively (Table 1, entries 6-8). Based on these results, 100 °C was selected as optimum temperature.

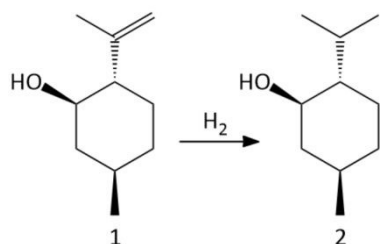
Finally, different experiments were performed at different flow rates (0.1, 0.2 and 0.3 mL min⁻¹) fixing the H₂ pressure at 30 bar and the temperature at 100 °C. The obtained yields to (–)-menthol were 91.3%, 57.9% and 48.0% using 0.1, 0.2, 0.3 mL min⁻¹ as flow rate (Table 1, entries 9-11).

Summarizing, 91.3% of yield was obtained using SCATs under optimum conditions (30 bar H₂ pressure, 100 °C and 0.1 mL min⁻¹), demonstrating the efficient activity of this system as catalyst.

The catalytic performance of SCATs was subsequently compared with commonly employed commercially available 30 mm-long cartridge ThalesNano CatCarts® containing 1%Pd/C (Table 1, entry 12). Surprisingly, SCATs showed almost comparable performances respect to commercially available 1%Pd/C (~94% of yield).

In a second phase, SCATs were charged in longer cartridges. Notably, hydrogenation reactions under continuous-flow are normally carried using 30 mm-long cartridge, as most of the catalysts are expensive or need time-consuming synthesis.⁴²⁻⁴⁷ However, the H-Cube® Mini Plus allows to use 70-mm long cartridge, less reported in literature.^{48, 49}

Table 1 Temperature (T), pressure (p), flow rate, residence time (τ) and yields at stationary state conditions (after 15') for the hydrogenations of (–)-isopulegol (1) to (–)-menthol (2).



Entry	Catalyst	p / bar	T / °C	Flow rate / mL min ⁻¹	τ / min	Yield / %
1	BLANK	30	100	0.1	3.8	<1
2	SCATs	10	100	0.1	3.8	40.2
3	SCATs	20	100	0.1	3.8	78.9
4	SCATs	30	100	0.1	3.8	91.3
5	SCATs	40	100	0.1	3.8	91.1
6	SCATs	30	75	0.1	3.8	55.5
7	SCATs	30	90	0.1	3.8	73.1
8	SCATs	30	100	0.1	3.8	91.3
9	SCATs	30	100	0.1	3.8	91.3
10	SCATs	30	100	0.2	1.9	57.9
11	SCATs	30	100	0.3	1.3	48.0
12*	1%Pd/C	30	100	0.1	3.8	94.2

Reaction parameters: (–)-isopulegol (20 mM in toluene). Yields to (–)-menthol were determined by GC using octane as internal standard. None of the tests led to the formation of by-products, achieving in all experiments 100% selectivity to (–)-menthol except for * where selectivity of 5.8% to sub products was detected by GC and GC-MS analysis.

Since SCATs are widely-available and cheap, it's possible to use them in larger quantities in order to implement and scale-up the catalytic performances by increasing the residence time.

For the reactions, 450 mg of SCATs were packed in 70 mm-long cartridge ThalesNano CatCarts®.

The tests were carried out operating at 30 bar H₂ pressure and 100 °C and varying the flow rates (Table 2, entries 2-5). At stationary state, (–)-menthol yields were 95.5%, 90.9%, 89.3% and 57.5% for 0.1, 0.3, 0.5 and 1.0 mL min⁻¹ flow rates, respectively. It is worth to point out that also the tests carried out at higher flow rates (0.3-0.5 mL min⁻¹) gave remarkable results, as showed in Table 2, entry 3 and 4, while for 30 mm long cartridges (less catalyst content) the yield sensibly already decreased at flow rates of 0.2 mL min⁻¹.

The catalytic performances of SCATs were also compared to the those of commercially available 70 mm-long cartridges ThalesNano CatCarts® containing 1%Pd/C (Table 2, entry 6) under previously optimized conditions. Remarkably, SCATs showed equal catalytic activities (95.5% yield) as compared to commercial 1%Pd/C (91.6% yield).

Table 2 Temperature (T), pressure (p), flow rate, residence time (τ) and yields at stationary state conditions (after 15'). DOI: 10.1039/C9GC04091A

Entry	Catalyst	p / bar	T / °C	Flow rate / mL min ⁻¹	τ / min	Yield / %
1	BLANK	30	100	0.1	8.8	<1
2	SCATs	30	100	0.1	8.8	95.5
3	SCATs	30	100	0.3	2.9	90.9
4	SCATs	30	100	0.5	1.8	89.3
5	SCATs	30	100	1.0	0.9	57.5
6*	1%Pd/C	30	100	0.1	8.8	91.6

Reaction parameters: (–)-isopulegol (20 mM in toluene). Yields to (–)-menthol were determined by GC using octane as internal standard. None of the tests led to the formation of by-products, achieving in all experiments 100% selectivity to menthol except for * where selectivity of 8.4% to sub products was detected by GC and GC-MS analysis.

Lastly, the long-term stability of SCATs was investigated under optimum continuous-flow conditions (p = 30 bar H₂; T = 100 °C; flow rate = 0.1 mL min⁻¹). The hydrogenation reaction was performed for a 6 h time-on-stream as illustrated in Fig. 3. After 2 h, a reduction of catalyst activity down to 85% of yield could be observed, while selectivity remained constant at 100%. No significant changes in the conversion of (–)-isopulegol were further observed for the successive 4-8 h. After a washing cycle, the activity was completely restored, proving that the decrease in the yield was most likely due to adsorption of substances on the active sites of the SCATs.

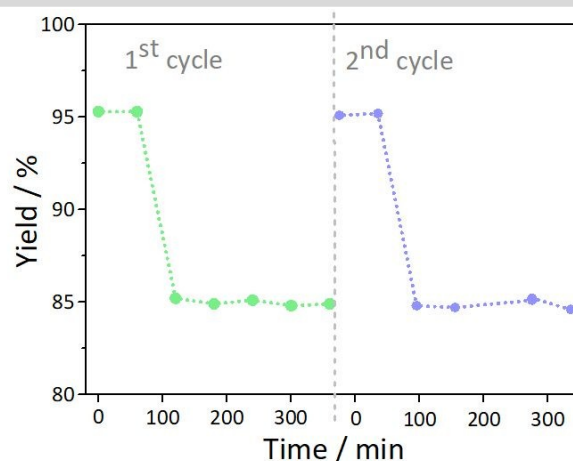


Fig. 3 Stability test of SCATs. Reaction conditions: p = 30 bar H₂; T = 100 °C; flow rate = 0.1 mL min⁻¹. The 2nd cycle of stability was performed after washing the SCATs of the 1st cycle with toluene for 10' with a flow rate = 2 mL min⁻¹.

Hydrogenation of (–)-isopulegol with the combined apparatus.

In order to study the effect of the temperature on the previous reaction, further hydrogenation experiments were performed in the combined apparatus (H-Cube®–X-Cube™). Indeed, the temperature of the H-Cube® equipment has operative limitations (maximum temperature 100 °C), while the utilization of the heating unit of the X-Cube™ allows to perform hydrogenations up to higher temperature.

Furthermore, the heat distribution inside the heating unit of the H-Cube® is not homogeneous, while the heating system of the X-Cube™ permits a more uniform heat distribution (please see Fig. S4 in the ESI for the photos of the two different heating units).

Washed and thermally treated SCATs were packed (450 mg of powder per cartridge) in 70 mm-long cartridge ThalesNano CatCarts®. Firstly, the hydrogenation of (–)-isopulegol was performed in the previous optimized conditions (30 bar H₂ pressure, 100 °C, 0.1 mL min^{–1}, 20 mM (–)-isopulegol in toluene) with the combined apparatus (Table 3, entry 1). The almost complete yield to menthol (>99.9%) in comparison with the previous obtained yield of 95% (Table 2, entry 2) suggested that the design of heating unit of the X-Cube™ allowed to homogeneously heat the entire cartridge.

Based on this encouraging result, a set of trials was conducted increasing the concentration of the starting material (Table 3, entries 1–3). The experiments were performed using 20, 50 and 100 mM solutions of (–)-isopulegol in toluene and all the tests provided challenging results, reaching almost complete conversions. Therefore, the starting solution of 100 mM of (–)-isopulegol was selected to accomplish further experiments for the optimization of other reaction parameters.

In details, a sequence of hydrogenations was performed increasing the flow rate from 0.1 up to 2 mL min^{–1} (Table 3, entries 4–8). A drop in the yields was observed. Since the reactions at 0.1, 0.3, 0.5 mL min^{–1} (Table 3, entry 4–6) were almost complete, while 1 mL min^{–1} of flow rate provided ~50% of yield (Table 3, entry 7), 1 mL min^{–1} was chosen for the following experiments carried out increasing the temperature from 100 to 170 °C (Table 3, entries 9–13).

Table 3 Temperature (T), pressure (p), flow rate, residence time (τ), concentration (c) and yields at stationary state conditions (after 15').

Entry	p / bar	T / °C	Flow rate / mL min ^{–1}	τ / min	c / mM	Yield / %
1	30	100	0.1	8.8	20	>99.9
2	30	100	0.1	8.8	50	>99.9
3	30	100	0.1	8.8	100	99.1
4	30	100	0.1	8.8	100	99.1
5	30	100	0.3	2.9	100	93.3
6	30	100	0.5	1.8	100	81.3
7	30	100	1.0	0.9	100	51.7
8	30	100	2.0	0.45	100	29.1
9	30	100	1.0	0.9	100	51.7
10	30	120	1.0	0.9	100	62.6
11	30	140	1.0	0.9	100	75.0
12	30	160	1.0	0.9	100	72.5
13	30	170	1.0	0.9	100	72.2
14*	30	140	1.0	0.9	100	81.0

None of the tests led to the formation of by-products, achieving in all experiments 100% selectivity to menthol, except for * (1%Pd/C) where selectivity of ~19% to sub products was detected by GC and GC-MS analysis.

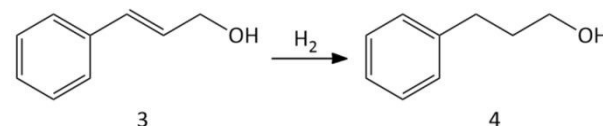
As expected, a higher temperature delivered a higher yield, with a maximum at 140 °C (Table 3, entry 11). Considering that the yields obtained (Table 3, entries 12–13) at 160 and 170 °C were almost the same obtained at 140 °C (~75%) (Table 3, entry 11), this last value was chosen as optimal temperature, in order to diminish the energy consumption.

Finally, the catalytic activity of SCATs was compared with that of commercial catalyst 1%Pd/C (Table 3, entry 14) under the optimized conditions. Despite a complete conversion of isopulegol was observed, a lower yield to menthol, in comparison with the reaction carried out at 100 °C (Table 2, entry 6) was noticed. Indeed, the higher temperature provided a higher production of sub products (e.g. menthone), less favored at lower temperature. However, the final yield was only 6% higher than the yield obtained with SCATs.

Hydrogenation of cinnamyl alcohol with the combined apparatus.

The hydrogenation of cinnamyl alcohol was initially investigated performing a sequence of experiments using different concentrations of the starting material (from 20 mM to 100 mM cinnamyl alcohol in toluene) (Table 4, entries 1–3). The trials conducted at 20 and 50 mM gave ~100% of yield (Table 4, entries 1–2), while a dramatic drop in yield (~46%) was obtained with the 100 mM solution (Table 4, entry 3). As a result, 50 mM solution was selected to conduct further experiments.

Table 4 Temperature (T), pressure (p), flow rate, residence time (τ), concentration (c) and yields at stationary state conditions (after 15') for the hydrogenations of cinnamyl alcohol (3) to hydrocinnamyl alcohol (4).



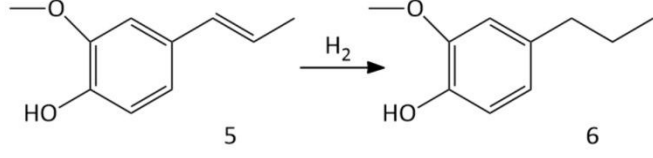
Entry	p / bar	T / °C	Flow rate / mL min ^{–1}	τ / min	c / mM	Yield / %
1	30	100	0.1	8.8	20	>99.9
2	30	100	0.1	8.8	50	>99.9
3	30	100	0.1	8.8	100	46.1
4	30	100	0.1	8.8	50	>99.9
5	30	100	0.3	2.9	50	64.8
6	30	100	0.5	1.8	50	63.5
7	30	100	1.0	0.9	50	32.8
8	30	100	2.0	0.45	50	12.5
9	30	100	0.5	1.8	50	63.5
10	30	120	0.5	1.8	50	70.0
11	30	140	0.5	1.8	50	77.2
12	30	160	0.5	1.8	50	78.8
13	30	170	0.5	1.8	50	77.4
14 *	30	140	0.5	1.8	50	98.8

None of the tests led to the formation of by-products, achieving in all experiments 100% selectivity to hydrocinnamyl alcohol; *test performed with commercial catalyst 1%Pd/C.

Successively, the hydrogenations were carried out varying the flow rate from 0.1 to 2 mL min⁻¹ (Table 4, entries 4-8). An increase in the flow rate delivered a lower yield. As the yield obtained at 0.1 mL min⁻¹ (Table 4, entry 4) was ~100%, while almost the same value of yields (~65%) were obtained operating with 0.3 and 0.5 mL min⁻¹ flow rate (Table 4, entries 5-6), 0.5 mL min⁻¹ was chosen for the following experiments at higher temperature (from 100 to 170 °C as reported in Table 4, entries 9-13). A higher temperature provided a higher yield, reaching a plateau at 140 °C and above (Table 4, entries 11-13). Commercially available 1%Pd/C was sequentially tested under the best operative conditions (Table 4, entry 14). In this case, the commercially available catalyst provided almost 20% higher yield to desired product.

Hydrogenation of isoeugenol with the combined apparatus. A set of trials for the hydrogenation of isoeugenol was initially performed using different concentrations of isoeugenol (from 20 mM to 100 mM in toluene) (Table 5, entries 1-3). The hydrogenations conducted at 20 and 50 mM gave almost complete conversions of isoeugenol (Table 5, entries 1-2), while ~93% of yield was obtained using the 100 mM solution (Table 5, entry 3). Successively, the flow rate was increased from 0.1 to 2 mL min⁻¹ (Table 5, entries 4-8).

Table 5 Temperature (T), pressure (p), flow rate, residence time (τ), concentration (c) and yields at stationary state conditions (after 15') for the hydrogenations of isoeugenol (5) to dihydroeugenol (6).



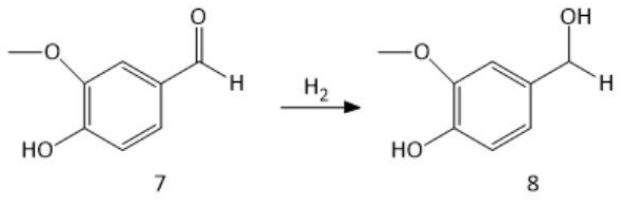
Entry	p / bar	T / °C	Flow rate / mL min ⁻¹	τ / min	c / mM	Yield / %
1	30	100	0.1	8.8	20	>99.9
2	30	100	0.1	8.8	50	97.4
3	30	100	0.1	8.8	100	92.7
4	30	100	0.1	8.8	100	92.7
5	30	100	0.3	2.9	100	59.6
6	30	100	0.5	1.8	100	35.6
7	30	100	1.0	0.9	100	22.7
8	30	100	2.0	0.45	100	17.0
9	30	100	0.3	2.9	100	59.6
10	30	120	0.3	2.9	100	61.4
11	30	140	0.3	2.9	100	69.6
12	30	160	0.3	2.9	100	71.2
13	30	170	0.3	2.9	100	71.5
14 *	30	140	0.3	2.9	100	80.8

None of the tests led to the formation of by-products, achieving in all experiments 100% selectivity to dihydroeugenol; *test performed with commercial catalyst 1%Pd/C.

An initial flow rate of 0.1 mL min⁻¹ (Table 5, entry 4) delivered a yield of ~100% while an increase in the flow up to 2 mL min⁻¹ produced a remarkable fall in yield (Table 5, entries 5-8). The flow rate of 0.3 mL min⁻¹ (yield to dihydroeugenol of ~60%) was chosen as optimum flow rate in order to investigate the influence of the temperature (from 100 to 170 °C, reported in Table 5, entries 9-13). A higher temperature provided a higher yield, with a maximum at 140 °C (Table 5, entry 11) and a plateau up to 170 °C (Table 5, entries 12-13). Under optimized reaction conditions, the reaction conducted using 1%Pd/C (Table 5, entry 14) provided 82% yield to final product. The commercially available catalyst showed only ~10% higher yield to dihydroeugenol, compared to SCATs.

Hydrogenation of vanillin with the combined apparatus. The first tests for the hydrogenation of vanillin to vanillyl alcohol were conducted varying the concentration of the starting material from 10 mM to 100 mM in toluene fixing the operative conditions at 30 bar H₂ pressure, 100 °C and 0.1 mL min⁻¹ flow rate (Table 6, entries 1-3). Due to the low activity, the flow rate was set to 0.1 mL min⁻¹ for all the following experiments, as trials at higher flux were considered unnecessary. A range of experiments were then conducted incrementing the temperature (Table 6, entries 4-8). As expected, a higher temperature delivered higher yields, reaching a maximum at 160 °C (Table 6, entry 7). Encouragingly, the reaction carried out under the best reaction conditions using commercial 1%Pd/C (Table 6, entry 9) showed almost a comparable yield to the one obtained with SCATs (57.3% and 50.1% respectively).

Table 6 Temperature (T), pressure (p), flow rate, residence time (τ), concentration (c) and yields at stationary state conditions (after 15') for the hydrogenations of vanillin (7) to vanillyl alcohol (8).

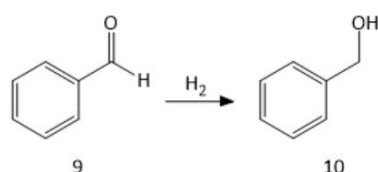


Entry	p / bar	T / °C	Flow rate / mL min ⁻¹	τ / min	c / mM	Yield / %
1	30	100	0.1	8.8	10	3.4
2	30	100	0.1	8.8	20	0
3	30	100	0.1	8.8	100	0
4	30	100	0.1	8.8	10	3.4
5	30	120	0.1	8.8	10	8.7
6	30	140	0.1	8.8	10	26.7
7	30	160	0.1	8.8	10	50.1
8	30	170	0.1	8.8	10	47.0
9 *	30	160	0.1	8.8	10	57.3

None of the tests led to the formation of by-products, achieving in all experiments 100% selectivity to vanillyl alcohol; *test performed with commercial catalyst 1%Pd/C.

Hydrogenation of benzaldehyde with the combined apparatus. The hydrogenation of benzaldehyde to benzyl alcohol was initially studied using a concentration of the starting material of 10 mM and 20 mM in toluene and fixing the reaction conditions at 30 bar H₂ pressure, 100 °C and 0.1 mL min⁻¹ flow rate (Table 7, entries 1-2). Sequentially, operating with the lower concentration, the temperature was increased up to 170 °C (Table 7, entries 3-7). Neither of the experiments showed appreciable yields. On the other hand, commercial 1%Pd/C was highly active for the reaction (Table 7, entry 8). The obtained results clearly demonstrated a low applicability of the SCATs for the hydrogenation of this biomass derived chemical.

Table 7 Temperature (T), pressure (p), flow rate, residence time (τ), concentration (c) and yields at stationary state conditions (after 15') for the hydrogenations of benzaldehyde (9) to benzyl alcohol (10).



Entry	p / bar	T / °C	Flow rate / mL min ⁻¹	τ / min	c / mM	Yield / %
1	30	100	0.1	8.8	10	10.9
2	30	100	0.1	8.8	20	3.2
3	30	100	0.1	8.8	10	10.9
4	30	120	0.1	8.8	10	10.3
5	30	140	0.1	8.8	10	10.7
6	30	160	0.1	8.8	10	9.5
7	30	170	0.1	8.8	10	10.4
8 *	30	100	0.1	8.8	10	94.2

None of the tests led to the formation of by-products, achieving in all experiments 100% selectivity to benzyl alcohol. *test performed with commercial catalyst 1%Pd/C

Stability tests. The long-term stability test of SCATs was performed in order to prove the stability of SCATs in the combined apparatus. Specifically, the hydrogenation of cinnamyl alcohol (77% yield in Table 4, entry 11) was selected as model reaction. The hydrogenation reaction was performed for a 15 h time-on-stream, as illustrated in Fig. 4.

Despite almost no changing in the yields to hydrocinnamyl alcohol was detected in the first 2 h, a reduction of catalyst activity of ~12% was observed after 3 h, reaching a plateau up to 15 h of reaction. A washing cycle was subsequently performed by pumping toluene in the continuous flow combined apparatus in order to check if the drop in the activity of the SCATs was due to the adsorption of materials on the surface of the catalysts rather than a deactivation. GC and GC-MS analysis of the fluxed and concentrated toluene showed the presence of the starting cinnamyl alcohol, confirming that the slight fall in reactivity after 15 h could be due to adsorbed starting compound on the surface of SCATs (please see Fig.S5 in the ESI for the graph reporting the GC-MS signal).

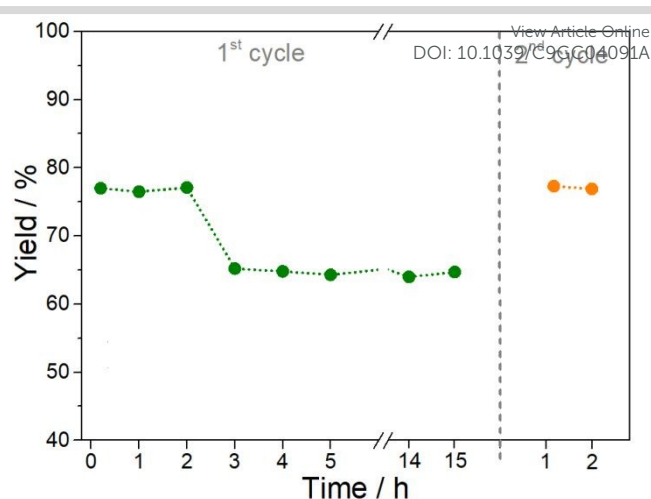


Fig. 4 Stability test of SCATs in the combined apparatus. Reaction conditions: p = 30 bar H₂; T = 140 °C; flow rate = 0.5 mL min⁻¹, 50 mM cinnamyl alcohol in toluene. The 2nd cycle of stability was performed after washing the SCATs of the 1st cycle with toluene for 10' with a flow rate = 2 mL min⁻¹.

ICP-MS analysis of the collected outcome toluene was also performed detecting no traces of metals, proving that no metal leaching occurred even under long term trials. Almost identical yields were observed in the second cycle.

Characterization after stability tests. Importantly, SCATs after long run experiment were fully characterised and compared to fresh washed and thermally treated SCATs.

Fig.5 shows STEM-HAADF analysis of SCATs after the catalytic tests. As reported in Fig. 5A and Fig. 5B, the metallic nanoparticles were still homogeneously distributed over the Al₂O₃ and SiO₂ surface. Fig. 5E shows the EDS analysis at four different locations, L4, L5, L6 and L7 in Fig. 5C, highlighting the presence of Ce and Pt nanoparticles. Remarkably, no relevant variations in morphology were observed. BET analysis showed a non-porous material with surface area of ~13 m² g⁻¹ before and after utilization (please see ESI Fig. S6 for isotherm graph of SCATs before utilization).

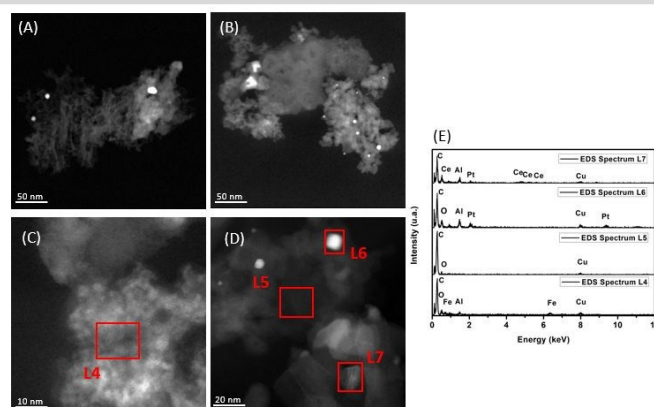


Fig. 5 SCATs after catalytic utilization (A), (B), (C) and (D) STEM-HAADF images, (E) EDS analysis of selected areas.

Neither leaching nor morphological variations were observed in the analysis of SCATs after reaction, showing a highly stable performance of the waste catalyst under continuous flow conditions. The observed slight initial deactivation is certainly due to the adsorption of organic compounds on the catalyst surface (as found by DRIFTS, results not shown). This hypothesis was confirmed by the fact that after a washing cycle, SCATs displayed the original catalytic activity, as shown in Fig. 5 "2nd cycle".

4. Conclusions

This work has demonstrated the applicability of a waste-derived material, scrap automotive catalytic converters (SCATs), in the continuous-flow hydrogenation of different biomass-derived chemicals. Remarkably, the SCATs showed comparable activity (only 6-10% less activity) to commercially available 1%Pd/C in the hydrogenations of isopulegol to menthol, isoeugenol to dihydroeugenol as well as in the hydrogenation of vanillin to vanillyl alcohol. Due to the easy preparation procedure (washing and thermal treatment) low-production of waste (calculated E-factor: ~20 §§§)⁵⁰, high activity, low price (up to 150 times less than commercial 1%Pd/C §§§§) SCATs have been proved to be efficient, environmentally-friendly, largely-available and cheap catalysts for continuous-flow hydrogenation reactions, paving the way to consider their application not only for the recovery of PGMs but also for the direct use as active components of catalytic system.

Conflicts of interest

The authors declare no conflicts of interest.

Acknowledgements

The authors thank Mr. Rafael Ángel Gómez Haro and Provaluta España Reciclaje de Metales, S.L., Córdoba (ES), for the supply of scrap automotive catalytic converters. Rafael Luque gratefully acknowledges MINECO for funding under project CTQ2016-78289-P, co-financed with FEDER funds and the contract for Camilla Maria Cova associated to this project. This project has received funding from the European Union's Horizon 2020 research and innovation programme under the Marie Skłodowska-Curie grant agreement No 721290. This publication reflects only the author's view, exempting the Community from any liability. Project website: <http://cosmic-etn.eu/>. The publication has been prepared with support from RUDN University program 5-100.

References

§ residence time (τ) = Catcarts volume / flow rate

§§ TOS: time on stream

§§§ E-Factor = total waste (kg) / product (kg). In details E-Factor= 2.0 kg/ 0.1 kg= 20

§§§§ According to prices available on <https://www.sigmaaldrich.com/>

- M. Selva and R. Luque, *Curr. Opin. Green Sust. Chem.*, 2019, **15**, 98-102.
- R. Luque, *Curr. Opin. Green Sust. Chem.*, 2016, **2**, 6-9.
- B. S. Kadu, A. M. Hengne, N. S. Biradar, C. V. Rode and R. C. Chikate, *Ind. Eng. Chem. Res.*, 2016, **55**, 13032-13039.
- C. Yu, J. J. Fu, M. Muzzio, T. L. Shen, D. Su, J. J. Zhu and S. H. Sun, *Chem. Mater.*, 2017, **29**, 1413-1418.
- J. Ni, W. H. Leng, J. Mao, J. G. Wang, J. Y. Lin, D. H. Jiang and X. N. Li, *App. Catal. B-Environ.*, 2019, **253**, 170-178.
- Directive 2000/53/EC of the European Parliament and of the Council of 18 September 2000, Official Journal of the European Communities, L269/34. Published: 21st October, 2000.
- C. Hagelucken, *Platin. Met. Rev.* 2012, **56**(1), 29-35.
- J. F. Weng, X. X. Lu and P. X. Gao, *Catalysts*, 2017, **7**(9), 253.
- J. Kaspar, P. Fornasiero and N. Hickey, *Catal. Today*, 2003, **77**, 419-449.
- A. Fornalczyk and M. Saternus, *Acta Metall. Sin-Engl.*, 2013, **26**, 247-256.
- D. J. de Aberasturi, R. Pinedo, I. R. de Larramendi, R. de Larramendi and T. Rojo, *Miner. Eng.*, 2011, **24**, 505-513.
- M. A. Barakat and M. H. H. Mahmoud, *Hydrometallurgy*, 2004, **72**, 179-184.
- C. H. Kim, S. I. Woo and S. H. Jeon, *Ind. Eng. Chem. Res.*, 2000, **39**, 1185-1192.
- M. K. Jha, J. C. Lee, M. S. Kim, J. Jeong, B. S. Kim and V. Kumar, *Hydrometallurgy*, 2013, **133**, 23-32.
- M. Baghalha, H. K. Gh and H. R. Mortaheb, *Hydrometallurgy*, 2009, **95**, 247-253.
- A. Fornalczyk, J. Willner, B. Gajda and J. Sedlakova-Kadukova, *Arch. Metall. Mater.*, 2018, **63**, 963-968.
- C. Saguru, S. Ndlovu and D. Moropeng, *Hydrometallurgy*, 2018, **182**, 44-56.
- N. Hodnik, C. Baldizzone, G. Polymeros, S. Geiger, J. P. Grote, S. Cherevko, A. Mingers, A. Zeradjanin and K. J. J. Mayrhofer, *Nat. Commun.*, 2016, **7**, 13164.
- H. Hasegawa, I. M. M. Rahman, Y. Egawa, H. Sawai, Z. A. Begum, T. Maki and S. Mizutani, *Water Air Soil Poll.*, 2014, **225**(9), 2112.
- M. Zengin, H. Genc, T. Demirci, M. Arslan and M. Kucukislamoglu, *Tetrahedron Lett.*, 2011, **52**, 2333-2335.
- H. Genc, *Catal. Commun.*, 2015, **67**, 64-67.
- E. Mieczynska, A. Gniewek and A. M. Trzeciak, *Appl. Catal. a-Gen.*, 2012, **421**, 148-153.
- F. Gomollón-Bel, *Chem. Int.*, 2019, **41**(2), 12-17.
- F. M. Akwi and P. Watts, *Chem. Commun.*, 2018, **54**, 13894-13928.
- L. Vaccaro, D. Lanari, A. Marrocchi and G. Strappaveccia, *Green Chem.*, 2014, **16**, 3680-3704.
- S. G. Newman and K. F. Jensen, *Green Chem.*, 2013, **15**, 1456-1472.
- C. Wiles and P. Watts, *Green Chem.*, 2012, **14**, 38-54.
- L. Rogers and K. F. Jensen, *Green Chem.*, 2019, **21** (13), 3481-3498.
- A. Hommes, H. J. Heeres and J. Yue, *Chemcatchem*, 2019, **11** (19), 4671-4708.
- G. Gralla, G. Heydrich, E. J. Bergner and K. Ebel, *US patent application Nr US*, 7960593, June, 2011.
- G. Heydrich, G. Gralla, M. Rauls, J. Schmidt-Leithoff, K. Ebel, W. Krause, S. Oehlenschläger, C. Jäkel, M. Friedrich, E. J. Bergner, J. Eike, N. Kashani-Shirazi and R. Paciello, *Spanish patent application Nr EP*, 07122036, November, 2007.
- J. Plosser, M. Lucas, J. Warna, T. Salmi, D. Y. Murzin and P. Claus, *Org. Process Res. Dev.*, 2016, **20**, 1647-1653.
- F. Iosif, S. Coman, V. Parvulescu, P. Grange, S. Delsarte, D. De Vos and P. Jacobs, *Chem. Commun.*, 2004, **11**, 1292-1293.

ARTICLE

Journal Name

- 34 Y. T. Nie, W. Niah, S. Jaenicke and G. K. Chuah, *J. Catal.*, 2007, **248**, 1-10.
- 35 A. M. Balu, J. M. Campelo, R. Luque and A. A. Romero, *Org. Biomol. Chem.*, 2010, **8**, 2845-2849.
- 36 V. I. Anikeev, I. V. Il'ina, K. P. Volcho and N. F. Salakhutdinov, *Russ. J. Phys. Chem. A*, 2012, **86**, 1917-1919.
- 37 C. Milone, C. Gangemi, G. Neri, A. Pistone and S. Galvagno, *Appl. Catal. a-Gen.*, 2000, **199**, 239-244.
- 38 A. F. Trasarti, A. J. Marchi and C. R. Apesteguia, *J. Catal.*, 2004, **224**, 484-488.
- 39 Y. T. Nie, S. Jaenicke and G. K. Chuah, *Chem-Eur. J.*, 2009, **15**, 1991-1999.
- 40 P. Maki-Arvela, J. Hajek, T. Salmi and D. Y. Murzin, *Appl. Catal. a-Gen.*, 2005, **292**, 1-49.
- 41 J.M.A. Harmsena, W.P.A. Jansenb, J.H.B. Hoebinka, J.C. Schoutena and H.H. Brongersmab, *Catal. Lett.*, 2001, **74** (3-4), 133-137.
- 42 J. M. Tukacs, R. V. Jones, F. Darvas, G. Dibo, G. Lezsak and L. T. Mika, *Rsc Adv.*, 2013, **3**, 16283-16287.
- 43 M. C. Bryan, D. Wernick, C. D. Hein, J. V. Petersen, J. W. Eschelbach and E. M. Doherty, *Beilstein J. Org. Chem.*, 2011, **7**, 1141-1149.
- 44 B. Szabo, B. Tamas, F. Faigl, J. Eles and I. Greiner, *J. Flow Chem.*, 2019, **9**, 13-17.
- 45 R. V. Jones, L. Godorhazy, N. Varga, D. Szalay, L. Urge and F. Darvas, *J. Comb. Chem.*, 2006, **8**, 110-116.
- 46 J. M. Tukacs, A. Sylvester, I. Kmecz, R. V. Jones, M. Ovari and L. T. Mika, *Roy. Soc. Open Sci.*, 2019, **6**(5), 182233.
- 47 E. Pfab, L. Filiciotto, A. A. Romero and R. Luque, *Ind. Eng. Chem. Res.*, 2019, **58**(35), 16065-16070.
- 48 C. Cazorla, M. Billamboz, H. Bricout, E. Monflier and C. Len, *Eur. J. Org. Chem.*, 2017, **6**, 1078-1085.
- 49 S. Sharma, Yamini and P. Das, *New J. Chem.*, 2019, **43**, 1764-1769.
- 50 R. A. Sheldon, *Chem. Ind.*, 1992, 903-906.

View Article Online
DOI: 10.1039/C9GC04091A